Optics and Laser Technology 127 (2020) 106167

Contents lists available at ScienceDirect

Optics and Laser Technology

journal homepage: www.elsevier.com/locate/optlastec

Near infrared broadband and visible upconversion emissions of erbium ions in oxyfluoride glasses for optical amplifier applications

Venkata Krishnaiah Kummara[a,*], Neelima G.[a,b], Ravi N.[a], Nanda Kumar Reddy Nallabala[c], Satish Kumar Reddy H.[a], Dwaraka Viswanath C.S.[d], Lenine D.[e], Surekha G.[a,b], Padma Suvarna R.[b], Yuvaraj C.[f], Venkatramu V.[g]

[a] Department of Physics, Rajeev Gandhi Memorial College of Engineering and Technology, Nandyal 518501, India
[b] Department of Physics, JNT University, Anantapuramu 515002, India
[c] Department of Physics, Madanapalle Institute of Technology and Science, Madanapalle 517 325, India
[d] Mother Theresa Institute of Engineering and Technology, Palamaner 517408, India
[e] Department of EEE, Rajeev Gandhi Memorial College of Engineering & Technology, Nandyal 518501, India
[f] Department of Mechanical Engineering, Madanapalle Institute of Technology & Science, Madanapalle, Chittoor 517325, India
[g] Department of Physics, Krishna University Dr. MRAR PG Centre, Nuzvid 521201, India

HIGHLIGHTS

- Erbium (Er^{3+})-doped oxyfluoride (PCfBfTiEr) glasses have been synthesized.
- Judd-Ofelt (JO) phenomenological intensity parameters (Ω_2, Ω_4, Ω_6) have been estimated.
- Intense eye-safe emission at 1534 nm has been obtained under 980 nm laser excitation.
- High emission cross-section and bandwidth product were obtained for PCfBfTiEr2.0 glass.

ARTICLE INFO

Keywords:
Oxyfluoro-phosphate glasses
Erbium ions
Optical band gap
Optical gain bandwidth
Decay curves
Lasers and amplifiers

ABSTRACT

Optical and visible upconversion properties of erbium (Er^{3+})-doped oxyfluoro-titania-phosphate glasses (PCfBfTiEr) with the chemical composition of P_2O_5–CaF_2–BaF_2–TiO_2–Er_2O_3 have been explored. An intense emission at 1.53 μm of Er^{3+}-doped PCfBfTiEr1.0 glass was obtained upon excitation of 980 nm diode laser. In addition, green and red visible upconversion emissions were obtained upon the optical excitation of Er^{3+} ions doped PCfBfTiEr glasses at 980 nm diode laser. Upconversion emission intensities and population densities of respective levels were tuned with the variation of Er^{3+} ion concentration. Fluorescence decay curves of the $^4I_{13/2}$ level of PCfBfTiEr glasses were obtained upon 980 nm laser excitation in the pulsed mode and revealed a mono-exponential behavior. The stimulated emission cross-section (σ_{em}), full width at half maximum (FWHM) and gain bandwidth product (σ_{em} × FWHM) were found to be 9.3 × 10^{-21} cm^2, 95.61 nm and 889.2 cm^{-2} nm for PCfBfTiEr2.0 glass, respectively. These results recommend that the Er^{3+} ions doped PCfBfTiEr glasses may possibly be worthy for the laser and optical amplification applications at 1.53 μm.

1. Introduction

Lanthanides (Ln^{3+}) doped glasses pay abundant attention for photonic applications due to their merits compared to crystalline materials that involve easy synthesis, low cost, produce a desired shape as well as size and consume less time for synthesis [1]. Among oxide glasses, phosphate glasses unveil several advantages due to the properties such as a low refractive index, good thermal and mechanical stabilities, high gain density, high transparency and relatively low melting temperature [2]. Phosphorus chain forms a bond easily with Ln^{3+} ions and transition metal ions to improve the luminescence properties. Ln^{3+} ions activated phosphate glasses have attracted many researchers to investigate suitable glass composition for the solid state lasers, memory switching, electrical threshold sensors and batteries because of wide technological applications [3].

Erbium (Er^{3+}) is the most substantial ion among the rest of the Ln^{3+}

* Corresponding author.
E-mail address: kvkphd84@gmail.com (V.K. Kummara).

https://doi.org/10.1016/j.optlastec.2020.106167
Received 27 August 2019; Received in revised form 3 January 2020; Accepted 24 February 2020

ions for 1.53 μm near infrared (NIR) lasers and optical amplifiers correspond to its emission transition of $^4I_{13/2} \rightarrow {}^4I_{15/2}$. Furthermore, Er^{3+} ion also shows emissions at the wavelengths of green and red are attributable to the $^2H_{11/2} + {}^4S_{3/2} \rightarrow {}^4I_{15/2}$ and $^4F_{9/2} \rightarrow {}^4I_{15/2}$ transitions respectively [4]. A large full width at half maximum (FWHM) of an emission band in the near infrared (NIR) region infers abundant prospective applications in optical amplifiers, waveguides and permitting for simultaneous traffic on quite a few channels of communication [5]. Er^{3+}-doped fiber amplifiers (EDFA) have played a vital role in optical communication for a long distances operated in the C-band region (1530–1565 nm). Furthermore, to extend the region of EDFAs in the prescribed region, Er^{3+} ions are essentially co-doped with other Ln^{3+} ions that includes Yb^{3+}, Tm^{3+}, Nd^{3+} and Pr^{3+} [6–9]. Present days, commercial EDFA uses silicate glasses for the fabrication of glass fibers which possess a narrow bandwidth of ~40 nm is then causing to limit broadband transmission. A suitable glass composition is substantial to be explored for the purpose of ultrabroadband EDFA applications [10]. Phosphate glasses are the right choice compared to other glasses for which chemical durability can be enhanced easily with the addition of heavy metal ions, Ba^{2+} and Ti^{4+} for the applications of ultrabroadband and high gain EDFA. Besides the oxide glasses, fluoride glasses have shown remarkable development for wide transparency from UV to IR, low Tg, low phonon energy and high fluorescence efficiency. Calcium fluoride (CaF_2) and barium fluoride (BaF_2) modifiers in the phosphate glass network can be used to achieve an efficient emission [11,12]. At present, researchers focusing on oxyfluoride glasses instead of conventional pure oxide glasses [13–15].

In the present study, Er^{3+}-doped (P_2O_5 + CaF_2 + BaF_2 + TiO_2 + Er_2O_3) PCfBfTiEr glasses were investigated in the perspective of high gain and broadband optical amplification. The mechanical strength of the phosphate network can be enhanced by the addition of TiO_2. An optical band gap, Urbach energy and dispersion of the glasses were estimated by the use of absorption spectrum. For 2.0 mol% Er^{3+} ions doped PCfBfTiEr2.0 glass, Judd-Ofelt (JO) intensity parameters were investigated to analyze the radiative properties such as radiative lifetime, the effective bandwidth, branching ratio and stimulated emission cross-section of the $^4I_{13/2} \rightarrow {}^4I_{15/2}$ transition for the emission band of Er^{3+} ion in the NIR region. Experimental lifetime of the metastable state, $^4I_{13/2}$ is estimated for different Er^{3+} ions concentration by fitting the luminescence decay curves with mono-exponential function. Finally, the results are compared with the other reported Er^{3+}-doped glasses.

2. Experimental techniques

2.1. Glass preparation

Glass samples were prepared by the conventional melt quenching technique [16] with the chemical composition of (60-*y*) P_2O_5 + 20 CaF_2 + 15 BaF_2 + 5 TiO_2 + *y*Er_2O_3 (*y* = 0.05, 0.1, 0.5, 1.0, 1.5, 2.0, 2.5 mol%) and the glasses labeled as PCfBfTiEr0.05, PCfBfTiEr0.1, PCfBfTiEr0.5, PCfBfTiEr1.0, PCfBfTiEr1.5, PCfBfTiEr2.0, PCfBfTiEr2.5, respectively. Phosphorus pentoxide (P_2O_5, 99.9%), calcium fluoride (CaF_2, 99.5%), barium fluoride (BaF_2, 99.9%), titanium dioxide (TiO_2, 99.9%) and erbium oxide (Er_2O_3, 99.8%) reagents from Alfa-Aesar and Sigma-Aldrich were used to prepare the glasses. Well mixture of powders about a batch of 15 gm placed into an alumina crucible for melting inside a super heat electric furnace at the temperature around 1300 °C for 90 min. The glass material was pivot on brass mold in the molten state and quenched suddenly to room temperature. The melt was cast onto a pre-heated brass mold and annealed at around 400 °C for 60 min below the glass transition temperature to release thermal stresses and strains of the glasses.

2.2. Characterization techniques

Fine polished Er^{3+}-doped PCfBfTiEr2.0 glass was used to extract the absorption spectrum using VARIAN Carry 5000 ultraviolet (UV)–visible–NIR double beam spectrophotometer in the absorbance mode. Photoluminescence spectra (visible up-conversion and NIR emission) and decay curves were obtained by 980 nm laser excitation in the continuous and pulse modes, respectively, by the use of visible as well as NIR detectors synchronized to Edinburg spectrofluorometer (FLS-980). Thickness (*t*) and density (ρ) of the PCfBfTiEr glass are 0.35 cm and 3.89 gm/cm^3, respectively. The refractive index of the glass was measured using J.A. Woollam Spectroscopic Ellipsometer (Model: M-2000VI) in the spectral range of 370–1690 nm with an error of ± 0.0023. Refractive index (*n*) of the glass was found to be 1.582 at a sodium wavelength. All the measurements were performed at room temperature.

3. Results and discussions

3.1. Optical absorption spectrum

Optical absorption spectrum of erbium (Er^{3+}) -doped PCfBfTiEr glasses were measured using UV–visible-NIR spectrometer in the region of 325–1800 nm at room temperature, as shown in Fig. 1(a) & (b). The absorption spectrum consist of twelve absorption peaks due to the transitions of Er^{3+} ions from the ground state ($^4I_{15/2}$) to different higher excited states labeled as $^4G_{9/2}$, $^4G_{11/2}$, $^2G_{9/2}$, $^4F_{3/2}$, $^4F_{5/2}$, $^4F_{7/2}$, $^2H_{11/2}$, $^4S_{3/2}$, $^4F_{9/2}$, $^4I_{9/2}$, $^4I_{11/2}$ and $^4I_{13/2}$. The optical absorption spectra show

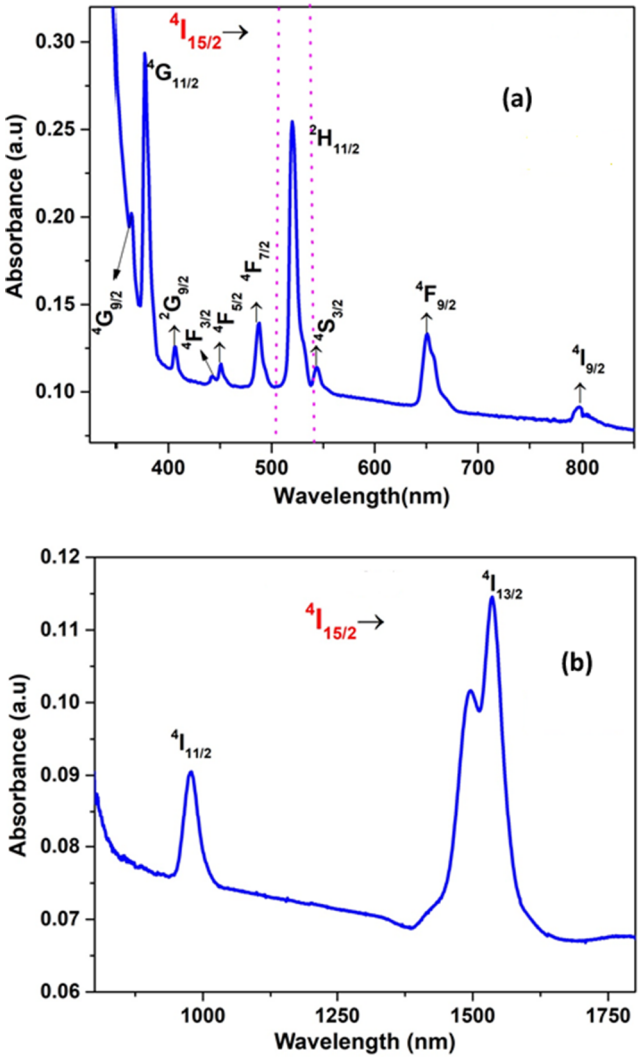

Fig. 1. Optical absorption spectrum of PCfBfTiEr2.0 glass in the (a) UV–visible (b) NIR regions.

Table 1
Optical absorption transitions, peak wavelength, corresponding energies and oscillator strengths (f_{exp} and f_{cal}) of Er^{3+}-doped PCfBfTiEr2.0 glass.

Wavelength (nm)	Wavenumber (cm^{-1})	Transitions, $^4I_{15/2}\rightarrow$	f_{exp}	f_{cal}	Δf
365	27,397	$^4G_{9/2}$	2.6400	2.4588	0.812
377	26,525	$^4G_{11/2}$	32.080	32.542	0.462
407	24,570	$^2G_{9/2}$	1.4600	1.4747	0.0147
443	22,537	$^4G_{3/2}$	0.8100	0.7036	0.1064
452	22,123	$^4G_{5/2}$	1.5810	1.2120	0.3690
487	20,491	$^4G_{7/2}$	4.1000	3.8919	0.2081
521	19,193	$^2H_{11/2}$	18.730	18.297	0.433
545	18,348	$^4S_{3/2}$	1.5100	0.9957	0.5143
652	15,337	$^4F_{9/2}$	3.6000	3.7584	0.1584
799	12,515	$^4I_{9/2}$	0.8200	0.5640	0.256
977	10,235	$^4I_{11/2}$	1.3800	1.3297	0.0503
1534	6523	$^4I_{13/2}$	2.5600	2.6283	0.0683
					δ_{rms} = **0.28**

highest intensity for the transitions $^4I_{15/2} \rightarrow {}^4G_{11/2}$ and $^4I_{15/2} \rightarrow {}^2H_{11/2}$ correspond to the peak positions at 377 nm and 520 nm, respectively. These transitions are "hypersensitive" transitions [17] which strongly reliant on covalence and the site symmetry of Er^{3+} ions and ligand. The hypersensitive transitions comply with the selection rules of $|\Delta S| = 0$, $|\Delta L| \leq 2$, $|\Delta J| \leq 2$ [18]. As a result, an intense absorption peak at a wavelength of 1534 nm for the PCfBfTiEr20 glass in the NIR region is shown in Fig. 1(b). The peak wavelengths of the optical absorption spectrum with their corresponding transitions and oscillator strengths were presented in the Table 1. The peak positions and profiles of Er^{3+} ion are analogous to other Er^{3+}-doped phosphate glasses that indicates as a uniform amalgamation of Er^{3+} ions in the glassy nature of local ligand fields [19].

3.2. Oscillator strengths (f_{exp} & f_{cal})

Absorption spectrum of PCfBfTiEr2.0 glass was used to find the oscillator strengths f_{exp} and f_{cal} for the electric-dipole transitions by least square fitting method from the JO theory. In this theory, the oscillator strength of the Er^{3+} ions is related to the intensity parameters Ω_λ (λ = 2, 4, 6). The intensity parameters were evaluated to understand the behavior of the electric-dipole and magnetic dipole strength of the ligand –Ln^{3+} ions within the glass matrix [20]. Among these parameters, Ω_2 is more subtle to the local structure of Er^{3+} ions and asymmetry. Ln^{3+} ion shows the degree of covalence and the polarizability of ligand ions in the glass matrices [21]. The Ω_6 is inversely proportional to the covalence of the Er-O bonds and is altered by the structure of the composition of the glass. Whereas Ω_4 be governed by the bulk properties of the glass, such as viscosity and rigidity of the bond as well as covalency between Er-O bonds [22]. Generally, Ω_4 and Ω_6 are mainly subjective to the acidity and alkalinity of glass. From the observations Ω_2 is larger in experimental oscillator strengths for Er^{3+}-doped glasses that includes phosphate, fluorophosphate, bismuth and borosilicate glasses [23–35]. It specifies that greater covalency between Er-O cause lopsidedness around Er^{3+} site however inferior covalency leads higher regularity in comparison with that of the other Er^{3+}-doped glasses.

The JO parameters for the PCfBfTiEr2.0 glass follows a trend of $\Omega_2 > \Omega_4 > \Omega_6$. However, compared with Ω_2 and Ω_4, Ω_6 is in a nominal structure which was erroneous sometimes. Ω_6 is the isomer shift with the relation of Ln^{3+} ions. This may be the result of hypersensitive transitions (HSTs) which follows the aforementioned selection rules. These HSTs are more intense and strong due to the ($4f^{11}$) Er^{3+} ion transitions, $^4I_{15/2} \rightarrow {}^4G_{11/2}$, and $^4I_{15/2} \rightarrow {}^2H_{11/2}$. The emission at 1.5 μm corresponds to $^4I_{13/2} \rightarrow {}^4I_{15/2}$ transition advantageous for laser and optical amplification applications which are owing to the magnetic and electric dipole interaction of the ligand ions (host glass). The spectroscopic quality factor ($\chi = \Omega_4/\Omega_6$) is an important parameter to anticipate the behavior of several lasing transitions in the glass matrix and is defined to quantify the Er^{3+} ions. For the PCfBfTiEr2.0 glass, the χ value is obtained as 0.99 and compared with the values of other reported Er^{3+}-doped glasses in Table 2. The quality factor is higher compared to 0.16 for 70.8 TeO_2–5 Al_2O_3–13 K_2O–(11-x) BaO–0.2 Er_2O_3 (TeAKBEr02) – tellurite glasses [26], 0.77 for (75-x) NaH_2PO_4–20 ZnO–5 Li_2CO_3– xEr_2O_3 (NZLE05) – sodium phosphate glasses [27], 0.86 for 50 ZrF_4–33 BaF_2–17 (LaF_3 + AlF_3 + YF_3)–1ErF_3 (ZBLAYEr10) – fluorozirconate glasses [30], 0.94 for 50 $(NaPO_3)_6$–10 TeO_2–20 AlF_3–19RF–1 Er_2O_3 (NaPTeALiEr10) – oxyfluoro sodium phosphate glasses [35] and 0.96 for 61 P_2O_5-13 BaO-10 Al_2O_3– 16 K_2O – xEr_2O_3 (BaKAPEr20) – barium phosphate glasses [33], but reported lower that include 1.03 for (46-x/2) P_2O_5-(46-x/2) Na_2O –8 B_2O_3 – x Er_2O_3 (PNaBEr05) - sodium phosphate glasses [25], 1.13 for 50 P_2O_5 –30 ZnO- 20 CdO (PZC03) – zinc phosphate glasses [24], 1.19 for 50 SiO_2 - (50-x) Na_2CO_3 - xEr_2O_3 (SiNaEr10) – sodium silicate glasses [29], 1.25 for 5 Na_2O–xSb_2O_3–(55-x) B_2O_3–39 SiO_2–1Er_2O_3 (NaSbBSiEr10) – borosilicate glasses [34], 1.39 for 99.5 (15 Ga_2O_3-75 GeO_2-10 R_2O) –0.5 Er_2O_3 (GeGaLEr05) gallium germinate glasses [31], 2.93 for 59 TeO_2–15 GeO_2–20 ZnO–5 K_2O–1Er_2O_3 (TGZKE10) – zinc tellurite glasses [28] and 7.07 for 60 SiO_2–10 GeO_2–10 B_2O_3–20 Na_2O – xEr_2O_3 (SiGeBNaEr10) - sodium silicate [32] glasses.

3.3. Optical bandgap

Tauc et al. [36] introduced a method to determine an optical bandgap from the optical absorption spectrum by drawing a plot between the absorbance and energy ($h\nu$). Later, Davis and Mott's [37] have been performed on amorphous germanium materials. According to them, optical absorption coefficient $\alpha(\nu)$ can be influenced by the photon energy ($h\nu$) and bandgap energy that follows:

Table 2
The Ω_λ parameters (λ = 2,4 and 6 × 10^{-22} cm^2), their trend and spectroscopic quality factor (χ) of Er^{3+}: glasses.

Glass matrix	Ref.	Ω_2	Ω_4	Ω_6	Trend	χ
PCfBfTiEr20	[PW]	3.23	2.63	2.61	$\Omega_2 > \Omega_4 > \Omega_6$	0.99
PZC03	[24]	1.23	0.77	0.68	$\Omega_2 > \Omega_4 > \Omega_6$	1.13
PNaBEr05	[25]	7.98	2.59	2.52	$\Omega_2 > \Omega_4 > \Omega_6$	1.03
TeAKBEr02	[26]	6.28	0.47	3.03	$\Omega_2 > \Omega_6 > \Omega_4$	0.16
NZLEr05	[27]	3.91	1.97	2.57	$\Omega_2 > \Omega_6 > \Omega_4$	0.77
TGZKE10	[28]	4.38	3.05	1.04	$\Omega_2 > \Omega_4 > \Omega_6$	2.93
SiNaEr10	[29]	1.19	0.31	0.26	$\Omega_2 > \Omega_4 > \Omega_6$	1.19
ZBLAYEr10	[30]	3.08	1.46	1.69	$\Omega_2 > \Omega_6 > \Omega_4$	0.86
GeGaLEr05	[31]	5.81	1.93	1.39	$\Omega_2 > \Omega_4 > \Omega_6$	1.39
SiGeBNaEr10	[32]	5.45	0.92	0.13	$\Omega_2 > \Omega_4 > \Omega_6$	7.07
BaKAPEr20	[33]	9.34	1.73	1.81	$\Omega_2 > \Omega_6 > \Omega_4$	0.96
NaSbBSiEr10	[34]	5.10	2.00	1.60	$\Omega_2 > \Omega_4 > \Omega_6$	1.25
NaPTeALiEr10	[35]	4.69	1.21	1.29	$\Omega_2 > \Omega_6 > \Omega_4$	0.94

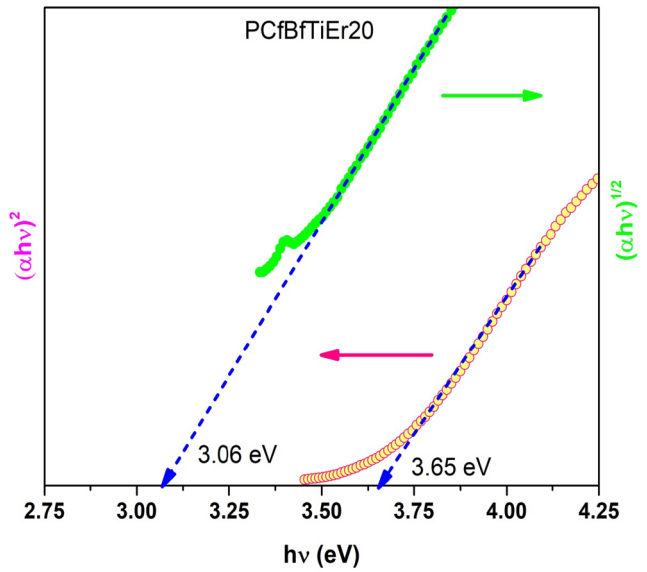

Fig. 2. Optical band gap representation for direct and indirect transitions of Er^{3+} ions doped PCfBfTiEr2.0 glass.

$$\alpha(\nu) = B\frac{(h\nu - E_g)^n}{h\nu} \quad (1)$$

where B is a constant, $h\nu$ is the energy of the photon and n is the index number generally used to characterize the type of electronic transition ($n = 2$ for direct whereas $n = 1/2$ for indirect allowed transitions). From the Fig. 2, the optical bandgap energy (E_g) is attained by the extrapolation of the linear portion of the curves to zero absorption i.e $(\alpha h\nu)^2 = 0$ and $(\alpha h\nu)^{1/2} = 0$ for allowed direct and indirect transitions, respectively [25].

The optical band gaps of PCfBfTiEr2.0 glass, both direct and indirect are estimated as 3.65 eV and 3.06 eV, respectively. The optical bandgap generally influenced not only by the chemical composition of the glass, but also affected by the local structure of the host matrix. This is due to the number of coordination of Er^{3+} ions at higher concentrations in the P_2O_5 network. The respective direct and indirect optical bandgaps are assessed in the range of 3.77–3.9 eV and 3.41–3.68 eV for PBEr0.5 glass [23], 4.57 eV indirect bandgap in the BAKAPEr20 glass [33].

Band tailing exists in the glass materials in the forbidden energy gap, which is a measure of the disorder of the glass that can be evaluated by the given Urbach formula

$$\alpha(h\nu) = \alpha_0 \exp\left[\frac{h\nu}{\Delta E}\right] \quad (2)$$

where α_0 is a constant and ΔE is the Urbach energy which is the width of the band tail of electronic states. Experimentally, ΔE is obtained by a plot drawn for $\ln(\alpha)$ against photon energy is as shown in Fig. 3. The origin of ΔE is due to the collection of the localized energy states below the conduction band, which is established as a result of the potential fluctuations in the glass. The exponential behavior of the curves observed in various materials is owing to the phonon-assisted indirect allowed electronic transitions. Skin depth (δ) is the measure of the penetration depth of the light through the glass before the incident beam scattered. The skin depth decreases with the increase of photon energy for Er^{3+}-doped PCfBfTiEr20 glass up to 4.17 eV and later it remains same, as presented in the Fig. 4. The Urbach energy of Er^{3+}-doped PCfBfTiEr2.0 glass is 0.29 eV, which is comparable with the other reported glasses.

3.4. Dispersion energy

Dispersion of energy plays a key role in optical materials in the applications of optical communication to design devices for spectral

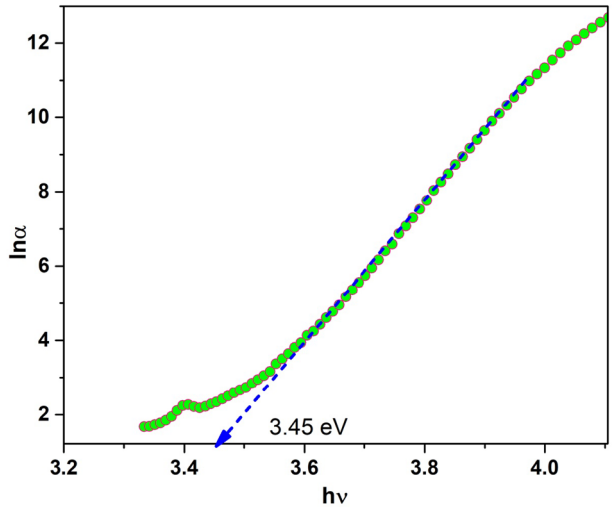

Fig. 3. The Urbach energy of Er^{3+} ions doped PCfBfTiEr2.0 glass for indirect allowed transitions.

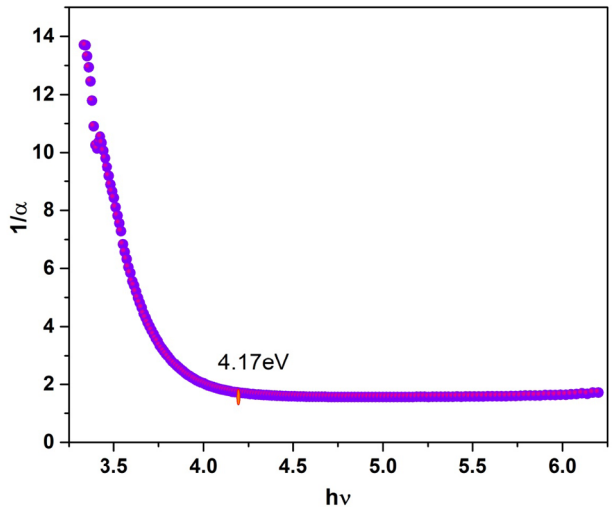

Fig. 4. Skin depth of the Er^{3+} ions doped PCfBfTiEr2.0 glass.

dispersion. Dispersion can be evaluated by the single-effective oscillator simulation suggested by Wemple and DiDomenico (the WDD model) [38]. The refractive index of the glass and the photon energy from the absorption can be understood by the following equation:

$$n^2 - 1 = \frac{E_0 E_d}{E_0^2 - E^2} \quad (3)$$

where n is the refractive index, E is the photon energy, E_0 is the effective oscillator strength directly related to the optical energy gap and E_d is the dispersion energy. A positive deviance in the curve from the linearity can be observed at smaller energies is subsequently of the negative impact of lattice vibrations to the refractive index. Conversely, negative deviance from the curve at higher energies is owing to the closeness of the band edge or excitonic absorption. The negative larger deviance from the linearity of Er^{3+}-doped PCfBfTiEr20 glass is the result of strong exciton peaks exist below the interband edge, as shown in the Fig. 5.

4. Photoluminescence (PL) emission spectra

PL spectra were recorded at room temperature upon excitation by 980 nm diode laser for different concentration of Er^{3+} ions in PCfBfTiEr glasses, as shown in Fig. 6(a). Emission spectra originated from the

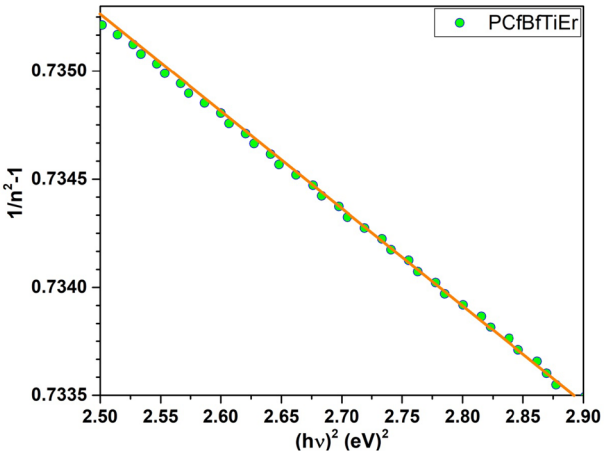

Fig. 5. Dispersion curve of the Er^{3+} ions doped PCfBfTiEr2.0 glasses.

meta-stable state to the ground state: $^4I_{13/2} \rightarrow {}^4I_{15/2}$ transition and an emission peak positioned at 1.53 μm in the NIR region. The emission intensity at 1.53 μm increases with increasing Er^{3+} ions concentration up to the 0.1 mol% doped PCfBfTiEr0.1 glass then decreased for PCfBfTiEr0.5 glass. A sudden increase in the emission intensity was found for the PCfBfTiEr1.0 glass and decreased for PCfBfTiEr1.5 glass. Therefore, it increases with the increase of Er^{3+} ion concentration up to the PCfBfTiEr2.5 glass. On the other hand, emission profile changes significantly and a red-shift was observed with the increase of Er^{3+} ion concentration. This shift may be due to reabsorption [39] as a result of the overlap of absorption and emissions. Moreover, the variation of integrated emission intensity with respect to Er^{3+} ions concentration is shown in Fig. 6(b). The full width at half maximum (FWHM) for the PCfBfTiEr1.5 glass is reported to be as high as 95.61 nm and compared with those of the other reported glasses [24–28,30–35,40,43]. It is observed that the FWHM was increased up to 66.07 nm for PCfBfTiEr0.5 glass, then suddenly decreased to 38.41 nm for PCfBfTiEr1.0 glass. Later, it is increased to 95.61 nm for PCfBfTiEr1.5 glass and decreased further with the increase of Er^{3+} concentration.

The gain bandwidth product (FWHM × σ_{em}) is a measure of the optical amplifiers for C, L band communication systems [40]. A high value of FWHM represents that the glasses could be a potential candidates for broadband amplification in a chirped-pulse amplification (CPA) band laser system which is a process for extremely high-energy laser pulses to manufacture cellphone screens.

5. Decay curve profile

Fig. 7. shows the decay curve profiles of the $^4I_{13/2}$ level of Er^{3+}-doped PCfBfTiEr glasses with respect to Er^{3+} ion concentration. The decay curves exhibit the mono-exponential behavior for all Er^{3+} ions concentration. Lifetime of $^4I_{13/2}$ level found to be 1.64, 2.11, 0.91, 1.34, 0.54, 0.54 and 0.65 ms for the PCfBfTiEr0.05, PCfBfTiEr0.1, PCfBfTiEr0.5, PCfBfTiEr1.0, PCfBfTiEr1.5, PCfBfTiEr2.0 and PCfBfTiEr2.5 glasses, respectively. The PCfBfTiEr0.1 glass has reported a highest lifetime of 2.11 ms compared with other investigated glasses. Lifetime (2.11 ms) of PCfBfTiEr0.1 glass was found higher than the other reported values of 0.81 ms for PKSAEr10 [10], 1.74 ms for BiPEr0.5 [19] and lower than 3.5 ms for PNaBEr05 [25] glasses. An increase in the lifetime of Er^{3+} ions at low concentration may be due to the absence of non-radiative losses such as energy transfer mechanisms. The decrease in the lifetimes of the $^4I_{13/2}$ level with an increase in Er^{3+} concentration is attributed to increase in non-radiative processes such as energy transfer among Er^{3+} ions that leads to luminescence quenching.

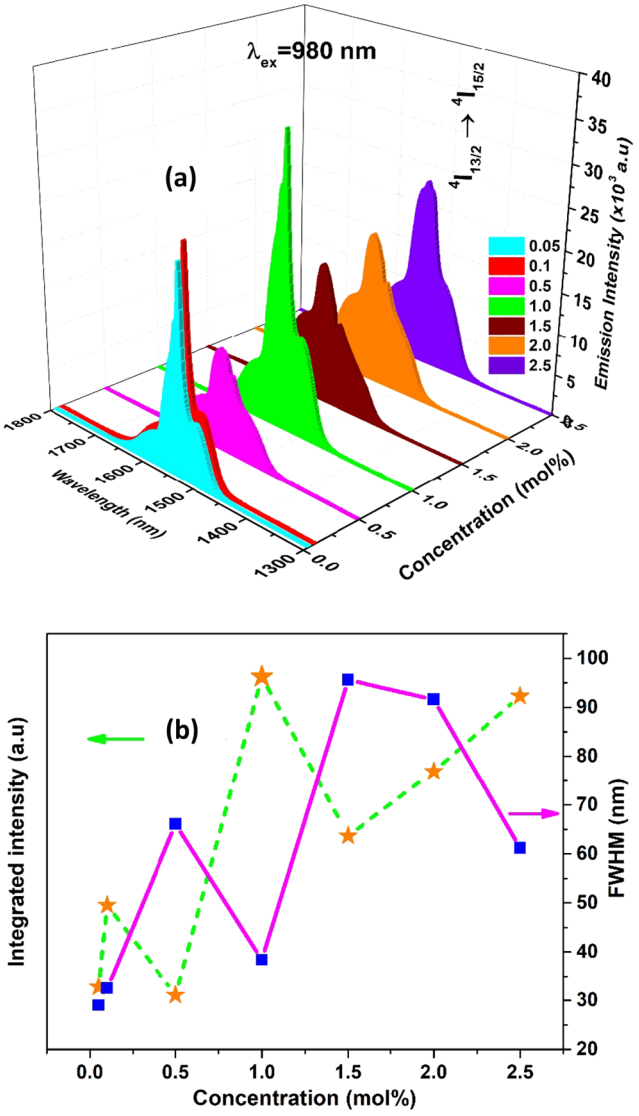

Fig. 6. (a) Emission spectra of Er^{3+}-doped PCfBfTiEr glasses for the $^4I_{13/2} \rightarrow {}^4I_{15/2}$ transition upon 980 nm diode laser excitation. (b) Variation of integrated intensity and FWHM for the $^4I_{13/2} \rightarrow {}^4I_{15/2}$ transition as a function of Er_2O_3 concentration.

6. Visible upconversion

Upon 980 nm excitation, green and red upconversion emissions of Er^{3+} were revealed and are presented in Fig. 8. The incident photon at 980 nm wavelength excites Er^{3+} ions to the $^4I_{11/2}$ level. A similar photon at 980 nm is used to excite Er^{3+} ions further via $^4I_{11/2} \rightarrow {}^4F_{7/2}$ transition. Then, the Er^{3+} ion relaxes rapidly to the $^2H_{11/2}$ level to yield emissions. Two emission bands were unveiled at 550 nm and 660 nm, correspond to the $^2H_{11/2} + {}^4S_{3/2} \rightarrow {}^4I_{15/2}$ (green) and $^4F_{9/2} \rightarrow {}^4I_{15/2}$ (red) transitions, respectively. Interestingly, at low Er^{3+} concentration (up to 0.5 mol%) the red emission is dominated and it changed to green at high Er^{3+} concentration (greater than equal to 1.0 mol%). The dominant red emission was resulted due to the population of Er^{3+} ions to the $^4F_{9/2}$ state because of the following processes: energy transfer (ET) between Er^{3+} ions among the levels $^4I_{13/2} + {}^4I_{11/2} \rightarrow {}^4I_{15/2} + {}^4F_{7/2}$, $^4I_{13/2} + {}^4I_{11/2} \rightarrow {}^4I_{15/2} + {}^4F_{9/2}$ and an excited state absorption (ESA) from the levels $^4I_{11/2} + h\nu \rightarrow {}^4F_{7/2}$, $^4F_{9/2}$. This indicates that the ET process is the prime reason for the up-conversion of red and green emissions. The variation of green emission intensity with the Er^{3+} ion concentration for PCfBfTiEr glasses revealed that the maximum

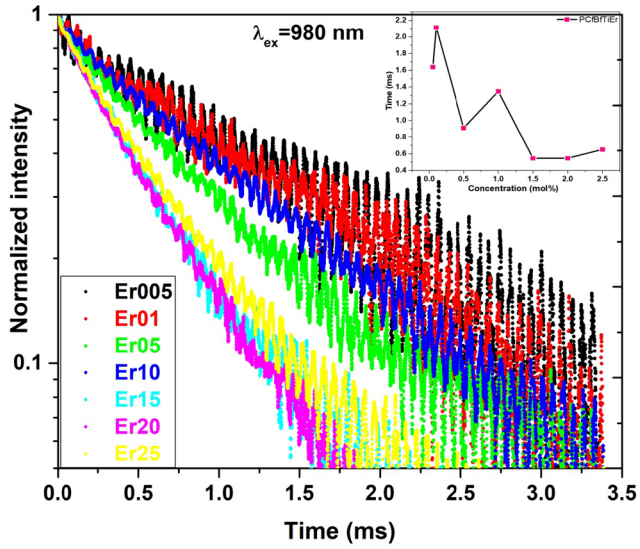

Fig. 7. Lifetime decay profiles of Er^{3+}-doped PCfBfTiEr glasses for the $^4I_{13/2} \rightarrow {}^4I_{15/2}$ transition upon pumped by 980 nm laser.

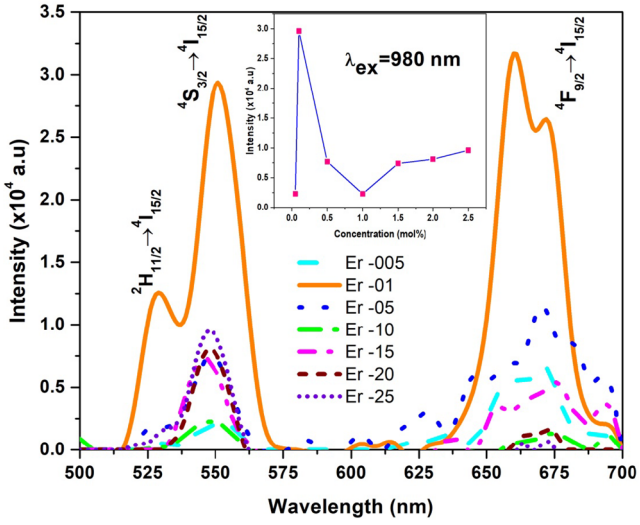

Fig. 8. Upconversion emission spectra of Er^{3+} ions in the PCfBfTiEr glasses upon 980 nm laser excitation. Inset shows the variation of up-conversion intensity as a function of Er_2O_3 concentration.

intensity attained for 0.1 mol% of Er^{3+}-doped PCfBfTiEr0.1 glass, as shown in the inset of Fig. 8. The green and red emissions of Er^{3+} ions can be understood through energy level diagram.

Fig. 9. shows the simplified energy level diagram of Er^{3+} doped PCfBfTiEr glasses under the excitation of 980 nm diode laser. When the Er^{3+} ions in the PCfBfTiEr glasses were excited by 980 nm diode laser, the Er^{3+} ions can be pumped to the higher energy state $^4I_{11/2}$ from the ground state $^4I_{15/2}$ due to ground state absorption (GSA: $^4I_{15/2} + h\nu \rightarrow {}^4I_{11/2}$). Moreover, these ions in the $^4I_{11/2}$ state may undergo an excited state absorption (ESA1: $^4I_{11/2} + h\nu \rightarrow {}^4F_{7/2}$) or the energy transfer upconversion (ETU1: $^4I_{11/2} + {}^4I_{11/2} \rightarrow {}^4F_{7/2} + {}^4I_{15/2}$) to pump the Er^{3+} ions to the $^4F_{7/2}$ level. Because of the less lifetime, these ions de-excite rapidly non-radiatively from the $^4F_{7/2}$ level to the meta stable states of Er^{3+} ions, $^2H_{11/2}$, $^4S_{3/2}$ and $^4F_{9/2}$ due to the small energy difference among them. As a result, green and red upconversion emissions were observed at 550 nm and 660 nm corresponds to the $^2H_{11/2} + {}^4S_{3/2} \rightarrow {}^4I_{15/2}$ and $^4F_{9/2} \rightarrow {}^4I_{15/2}$ transitions, respectively. The population among the levels can be altered with the variation of Er^{3+} ions concentration in these glasses (see Fig. 8). Based on the population

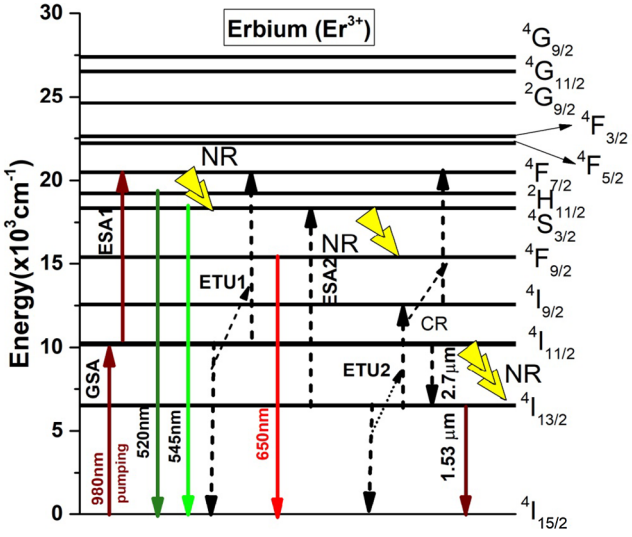

Fig. 9. Partial energy level diagram of Er^{3+} ions doped PCfBfTiEr glasses.

density, intensity of green and red emissions can be modified. Green and red emission intensities are varied quite contrary to each other with the variation of Er^{3+} ion concentration. The Er^{3+} ions can relax radiatively or non-radiatively from the $^4I_{11/2}$ level to $^4I_{13/2}$, in the case of radiative transition whose wavelength equal to 2.7 μm. Consequently, these ions relax to the ground state due to the $^4I_{13/2} \rightarrow {}^4I_{15/2}$ transitions through the emission with a well-known eye-safe wavelength of 1.53 μm. In addition to these transitions, ETU2: ($^4I_{13/2} + {}^4I_{13/2} \rightarrow {}^4I_{15/2} + {}^4I_{9/2}$) from $^4I_{9/2}$ and $^4I_{13/2}$ level, including the ESA2 of Er^{3+} ions, the $^4S_{3/2}$ and the $^4I_{13/2}$ levels can be populated which cause the up-conversion phenomena in Er^{3+}–doped glasses [40,41].

7. McCumber's theory

With the use of absorption spectrum, the emission cross-section at 1.53 μm corresponds to the transition $^4I_{13/2} \rightarrow {}^4I_{15/2}$ as a function of wavelength has been evaluated by the McCumber's theory using the given equation.

$$\sigma_e^m = \sigma_a \exp\left(\frac{\varepsilon - h\nu}{kT}\right). \tag{4}$$

where ε is the net-free energy used to excite Er^{3+} ions for the $^4I_{15/2} \rightarrow {}^4I_{13/2}$ transition at absolute temperature T, ν is the frequency of the emission band and k is the Boltzmann's constant. For PCfBfTiEr2.0 glasses, the absorption and emission cross-sections were calculated and their correlation is shown in Fig. 10. The absorption cross-section for the $^4I_{15/2} \rightarrow {}^4I_{13/2}$ transition is found to be 8.30×10^{-21} cm^2 whereas the emission cross-section of 9.3×10^{-21} cm^2 for the $^4I_{13/2} \rightarrow {}^4I_{15/2}$ transition. The σ_{abs} and σ_{em} endorses that the energy transfer from the excited to non-excited Er^{3+} ions because of the resonant processes. In the ground state, the unexcited Er^{3+} ions can absorb the emitted photons and stimulate to the excited state, then they emit the absorbed photons via de-excitation processes, which results the emission at different wavelengths. Consequently, the attained spectral shape of σ_{em} of the Er^{3+}-doped glasses useful for the wide range of telecommunication and moreover for the three level laser systems. The results reveal that for wavelengths shorter than the peak wavelength (λ_p), σ_{abs} is larger than the σ_{em} whereas for higher wavelengths the σ_{em} is larger.

The key radiative parameters such as σ_{em}, FWHM and gain bandwidth product of PCfBfTiEr2.0 glass are compared with the other reported Er^{3+}–doped glasses in the Table 3. Gain bandwidth or figure of merit (FOM) is the product of full width at half maximum (FWHM) and stimulated emission cross–section (FWHM × σ_{em}) is attained as high as 889.2 cm^{-2} nm for Er^{3+} doped PCfBfTiEr2.0glass compared to the

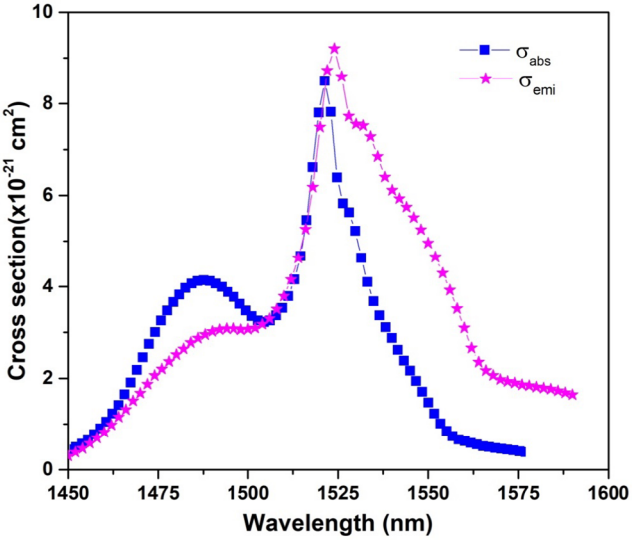

Fig. 10. The absorption (σ_{ab}) and emission cross-sections (σ_{em}) of $^4I_{13/2} \leftrightarrow {}^4I_{15/2}$ transitions for PCfBfTiEr2.0 glass.

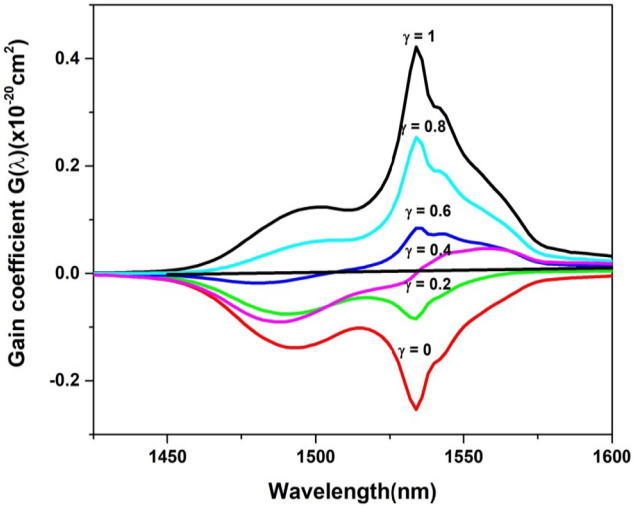

Fig. 11. Gain cross-section spectra of Er^{3+}-doped PCfBfTiEr2.0 glasses for the $^4I_{13/2} \rightarrow {}^4I_{15/2}$ transition.

other reported glasses that includes 337.5 for sodium phosphate (NZLEr05) [27], 424.01 for gallogermanate (GeGaLEr05) [31], 427.9 for sodium fluorophosphate (NaPTeALiEr10) [35], 497.6 for boro-sodiumphosphate (PNaBEr05) [25], 527.25 for bismuth-borogallate (BiBGaEr50) [42] and 598.4 for borosilicate (NaSbBSiEr10) [34] glasses. Using JO parameters, the evaluated radiative properties such as radiative transition probabilities (A_R), and radiative lifetimes (τ_R) are presented in the Table 3 along with the other reported Er^{3+}:glasses.

The product of FWHM and σ_{em} for the $^4I_{13/2} \rightarrow {}^4I_{15/2}$ transition is usually used to measure the gain bandwidth of an optical amplifier. Furthermore, at room temperature gain cross-section can be estimated by the equation:

$$G(\lambda, p) = \gamma\sigma_{em} - (1-\gamma)\sigma_{ab} \quad (5)$$

where γ is the population inversion rate, with an increment of 0.2 (γ = 0.0, 0.2, 0.4, 0.6, 0.8 and 0.1), σ_{abs} and σ_{em} are the absorption and emission cross-sections, respectively. The Fig. 11 displays gain cross-section spectra as a function of inverted population rate. From the spectra, it is perceived that the gain is positive in the wavelength range of 1530–1600 nm for the population inversion of 40%. With increase of population inversion, the gain is extracted and extended towards shorter wavelength from 1450 to 1600 nm. The peak of the gain cross-section spectrum switches toward shorter wavelengths as the population inversion increases [43].

8. Conclusion

Er^{3+}-doped PCfBfTiEr glasses with different Er^{3+} ion concentrations have been fabricated and characterized their optical and photoluminescence properties for optical amplification applications. Judd-Ofelt (JO) intensity parameters and radiative parameters were evaluated. The Ω_2 is relatively higher value which indicates higher covelance and/or higher asymmetry of Er^{3+} ion doped PCfBfTiEr glasses and compared to the other phosphate, silicate, tellurite and germinate glasses. The eye-safe emission at 1534 nm was obtained due to the $^4I_{13/2} \rightarrow {}^4I_{15/2}$ transition of Er^{3+} ions under 980 nm diode laser excitation. Upconversion emission at green and red regions corresponds to the $^2H_{11/2} + {}^4S_{3/2} \rightarrow {}^4I_{15/2}$ and $^4F_{9/2} \rightarrow {}^4I_{15/2}$ transitions, respectively, observed upon 980 nm diode laser excitation. Emission intensities of green and red upconversion emissions and population density of respective levels were altered with the Er^{3+} ions concentration. The FWHM, stimulated emission cross-section (σ_{em}), and gain bandwidth (FWHM × σ_{em}) for the $^4I_{13/2} \rightarrow {}^4I_{15/2}$ transition were found to be 95.61 nm, 9.3 × 10^{-21} cm^{-2} and 889.2 cm^{-2}nm, respectively. Decay curve analysis exposed that the lifetime of the $^4I_{13/2}$ level of Er^{3+} ion decreases with increase in Er^{3+} ion concentration. All the results show that the 2.0 mol% Er_2O_3 doped oxyfluoro-phosphate glasses could be a suitable candidates for broadband amplification in a chirped-pulse amplification (CPA) based laser systems.

Table 3
Comparison of peak wavelength, radiative transition probability, radiative lifetime, stimulated emission cross section ($\sigma_{em,} \times 10^{-21}$ cm^2), full width at half maximum (FWHM) and gain bandwidth (FWHM × σ_{em}) of Er^{3+}-doped glasses.

Glass matix	Ref.	λ_p nm	A_R s^{-1}	τ_R ms	σ_{em} (cm^2)	FWHM nm	Gain bandwidth (FWHM × σ_{em})
PCfBfTiEr20	[PW]	1534	68	14.7	9.3	95.61	889.2
PZC03	[24]	1538	770	1.2	4.7	–	——
PNaBEr05	[25]	1532	217	4.6	15.6	31.9	497.6
TeAKBEr02	[26]	1529	521	1.9	28.4	—	——
NZLEr05	[27]	1550	132	7.5	7.7	43	331.1
TGZKE10	[28]	1531	252	3.9	8.1	—	—
ZBLAYEr10	[30]	1550	155	6.5	9.2	—	—
GeGaLEr 05	[31]	1530	—	—	7.8	54.5	425.1
SiGeBNaEr10	[32]	1535	49	20.4	5.5	—	——
NaSbBSiEr10	[34]	1533	59	16.9	6.8	88	598.4
NaPTeALiEr10	[35]	1534	146	6.8	11.3	38	429.4
BiBGaEr50	[43]	1556	——	—	7.03	75	527.25

CRediT authorship contribution statement

Venkata Krishnaiah Kummara: Writing - original draft, Conceptualization, Formal analysis, Writing - review & editing. **Neelima G.:** Writing - original draft, Conceptualization, Formal analysis, Writing - review & editing. **Ravi N.:** Writing - original draft, Conceptualization, Formal analysis, Writing - review & editing. **Nanda Kumar Reddy Nallabala:** Writing - review & editing. **Satish Kumar Reddy H.** Formal analysis, Writing - review & editing. **Dwaraka Viswanath C.S.:** Formal analysis, Writing - review & editing. **Lenine D.:** Writing - review & editing. **Surekha G.:** Methodology, Writing - review & editing. **Padma Suvarna R.:** Writing - review & editing. **Yuvaraj C.:** Writing - review & editing. **Venkatramu V.:** Writing - original draft, Conceptualization, Formal analysis, Writing - review & editing.

Declaration of Competing Interest

The authors declare that they have no known competing financial interests or personal relationships that could have appeared to influence the work reported in this paper.

Acknowledgement

Dr. K.Venkata Krishnaiah is obliged to SERB-DST, New Delhi for sanctioning a research project (File Number: EMR/2017/000009). One of the authors Venkatramu is grateful to DST, New Delhi for the sanction of collaborative research project (No. INT/PORTUGAL/P-04/2017) under India-Portugal Bilateral Scientific and Technological Cooperation. The authors thankful to Prof. C.K. Jayasankar, Department of Physics, Sri Venkateswara University, Tirupati for supporting the PL experimental facility. Dr. N. Nanda Kumar Reddy and C. Yuvaraj thankfully acknowledges the financial support received from the DST Project No. ECR/2017/002868, DST-FIST Program-2015 (SR/FST/College-263) and MITS/TEQIP-II/FACULTY-SEED GRANT/19-20.

References

[1] S.Y. Moustafa, M.R. Sahar, S.K. Ghoshal, Erbium ions oscillator strength and emission enhancement in antimony phosphate amorphous matrix, J. Non Cryst. Solids 433 (2016) 87–94.
[2] P.Y. Shih, Thermal, chemical and structural characteristics of erbium-doped sodium phosphate glasses, Mater. Chem. Phys. 84 (2004) 151–156.
[3] I. Soltani, S. Hraiech, K. Horchani-Naifer, J. Massera, L. Petit, M. Férid, Thermal, structural and optical properties of Er^{3+} doped phosphate glasses containing silver nanoparticles, J. Non-Cryst. Solids 438 (2016) 67–73.
[4] Rolindes Balda, Noha Hakmeh, Macarena Barredo-Zuriarrain, Odile Merdrignac-Conanec, M. Sara García-Revilla, Angeles Arriandiaga, Joaquín Fernández, Influence of upconversion processes in the optically-induced inhomogeneous thermal behavior of erbium-doped lanthanum oxysulfide powders, Materials 9 (5) (2016) 353.
[5] Fausto M. Faria Filho, Rogéria R. Goncalves, Sidney J.L. Ribeiro, Lauro J.Q. Maia, Structural and optical properties of Er^{3+} doped SiO_2–Al_2O_3–GeO_2 compounds prepared by a simple route, Mater. Sci. Eng. B 194 (2015) 21–26.
[6] G.S. Li, C.M. Zhang, P.F. Zhu, C. Jiang, P. Song, K. Zhu, Broadband near-infrared emission in Pr^{3+}–Er^{3+} codoped phosphate glasses for optical amplifiers, Ceram. Int. 42 (2016) 5558–5561.
[7] Qun Han, Wenchuan Yan, Yunzhi Yao, Yaofei Chen, Tiegen Liu, Optimal design of Er/Yb co-doped fiber amplifiers with an Yb-band fiber Bragg grating, Photon. Res. 4 (2) (2016) 53–56.
[8] Grzegorz Sobon, Pawel Kaczmarek, Krzysztof M. Abramski, Erbium–ytterbium co-doped fiber amplifier operating at 1550 nm with stimulated lasing at 1064 nm, Opt. Commun. 285 (7:1) (2012) 1929–1933.
[9] Itai Ron Amos, A. Hardy, Neodymium, erbium, and ytterbium co-doped fiber amplifier, Opt. Eng. 50 (7) (2011) 074201.
[10] K. Linganna, M. Rathaiah, N. Vijaya, Ch. Basavapoornima, C.K. Jayasankar, S. Ju, W.-T. Han, V. Venkatramu, 1.53 mm luminescence properties of Er^{3+}-doped K-Sr-Al phosphate glasses, Ceram. Int. 41 (4) (2015) 5765–5771.
[11] Kaushik Biswas, Sathravada Balaji, Debarati Ghosh, Annapurna Kalyandurg, Enhanced near-infrared to green upconversion from Er^{3+}-doped oxyfluoride glass and glass ceramics containing $BaGdF_5$ nanocrystals, Int. J. Appl. Glass Sci. (2016) 1–13.
[12] Daniel Hahn, Calcium fluoride and barium fluoride crystals in optics, Optik Photonik (2015) 45–48.
[13] Ya-Pei Peng, Chuanfeng Wang, Xinqiang Yuan, Long Zhang, Er^{3+}-doped oxyfluorogallate glass for 2.7 μm solid-state lasers, J. Lumin. 172 (2016) 331–334.
[14] Marcin Środa, Katarzyna Cholewa-Kowalska, Marek Rózanski, Marek Nocun, Framework influence of erbium doped oxyfluoride glasses on their optical properties, Opt. Mater. 33 (2011) 397–401.
[15] M.H. Imanieh, I.R. Martín, J. Gonzalez-Platas, B. Eftekhari Yekta, V.K. Marghussian, S. Shakhesi, Behavior of Yb^{3+} and Er^{3+} during Heat treatment in oxyfluoride glass ceramics, J. Nanomater. (2014) 1–10.
[16] G. Neelima, K. Venkata Krishnaiah, N. Ravi, K. Suresh, K. Tyagarajan, T. Jayachandra Prasad, Investigation of optical and spectroscopic properties of neodymium doped oxyfluoro-titania-phosphate glasses for laser applications, Scr. Mater. 162 (2019) 246–250.
[17] C.R. Kesavulu, V.B. Sreedhar, C.K. Jayasankar, K. Jang, D.-S. Shin, S.S. Yi, Structural, thermal and spectroscopic properties of highly Er^{3+}-doped novel oxyfluoride glasses for photonic application, Mater. Res. Bull. 51 (2014) 336–344.
[18] B.R. Judd, Optical absorption intensities of rare-earth ions, Phys. Rev. 127 (3) (1962) 750–761.
[19] S. Damodaraiah, V. Reddy Prasad, Y.C. Ratnakaram, Investigation of Green and 1.53 μm emission characteristics of Er^{3+} doped bismuth phosphate glasses for laser applications, J. Alloys Compounds 741 (2018) 269–280.
[20] Yu Xiaochen, Feng Song, Wentao Wang, Lanjun Luo, Lin Han, Zhenzhou Cheng, Tongqing Sun, Jianguo Tian, Edwin Y.B. Pun, Comparison of optical parameters and luminescence between Er^{3+}/Yb^{3+} co doped phosphate glass ceramics and precursor glasses, J. Appl. Phys. 104 (2008).
[21] Fengxiao Wang, Feng Song, Shuangxin An, Wenshun Wan, Hao Guo, Shujing Liu, Jianguo Tian, Er^{3+}/Yb^{3+}-codoped phosphate glass for short-length high-gain fiber lasers and amplifiers, 1198, Appl. Opt. 54 (5) (2015) 1198–1205.
[22] K. Linganna, K. Suresh, S. Ju, W.-T. Han, C.K. Jayasankar, V. Venkatramu, Optical properties of Er^{3+}-doped K-Ca-Al fluorophosphate glasses for optical amplification at 1.53 μm, Opt. Mater. Express 1689 (2015) 1689–1703.
[23] A. Amarnath Reddy, S. Surendra Babu, K. Pradeesh, C.J. Otton, G. Vijaya Prakash, Optical properties of highly Er^{3+}-doped sodium–aluminium–phosphate glasses for broadband 1.5 m emission, J. Alloy. Compd. 509 (2011) 4047–4052.
[24] B. Afef, Moteb M. Alqahtani, H.H. Hegazy, E. Yousef, K. Damak, R. Maâlej, Green and near infrared emission of Er^{3+} doped PZS and PZC glasses, J. Lumin. 194 (2018) 706–712.
[25] S. Hraiech, C. Bouzidi, M. Férid, Luminescence properties of Er^{3+}-doped phosphate glasses, Physica B 522 (1) (2017) 15–21.
[26] J.J. Leal, R. Narro-García, H. Desirena, J.D. Marconi, E. Rodríguez, K. Linganna, E. dela Rosa, Spectroscopic properties of tellurite glasses co-doped with Er^{3+} and Yb^{3+}, J. Luminescence 162 (2015) 72–80.
[27] A. Langar, C. Bouzidi, H. Elhouichet, M. Férid, Er-Yb codoped phosphate glasses with improved gain characteristics for an efficient 1.55 mm broadband optical amplifiers, J. Lumin. 148 (2014) 249–255.
[28] Yanyan Guo, Ying Tian, Liyan Zhang, Hu. Lili, Junjie Zhang, Erbium doped heavy metal oxide glasses for mid-infrared laser materials, J. Non-Cryst. Solids 377 (2013).
[29] E.O. Serqueira, R. Ferreira de Morais, N.O. Dantas, Controlling the spectroscopic parameters of Er^{3+}-doped sodium silicate glass by tuning the Er_2O_3 and Na_2O concentrations, J. Alloys Compd. 560 (2013) 200–207.
[30] Y. Tian, R. Xu, L. Hu, J. Zhang, Spectroscopic properties and energy transfer process in Er^{3+} doped ZrF_4-based fluoride glass for 2.7 μm laser materials, Opt. Mater. 34 (2011) 308–312.
[31] D.M. Shi, Y.G. Zhao, X.F. Wang, G.H. Liao, C. Zhao, M.Y. Peng, Q.Y. Zhang, Effects of alkali ions on thermal stability and spectroscopic properties of Er^{3+}-doped gallogermanate glasses, Phys. B 406 (2011) 628–632.
[32] Qiuling Chen, Qiuping Chen HuiWang, Spectroscopic study of high Er and Er/Yb concentration doped photosensitive silicate glasses for integrated optics application, J. Non-Cryst. Solids 391 (2014) 43–48.
[33] R. Lachheb, A. Herrmann, A.A. Assadi, K. Damak, C. Rüssel, R. Maâlej, Judd- Ofelt analysis and experimental spectroscopic study of erbium doped phosphate glasses, J. Lumin. 201 (2018) 245–254.
[34] Q. Qian, Y. Wang, Q.Y. Zhang, G.F. Yang, Z.M. Yang, Z.H. Jiang, Spectroscopic properties of Er^{3+}-doped Na_2O–Sb_2O_3–B_2O_3–SiO_2 glasses, J. Non-Cryst. Solids 354 (2008) 1981–1985.
[35] M. Jayasimhadri, L.R. Moorthy, K. Kojima, K. Yamamoto, Noriko Wada, Noriyuki Wada, Er^{3+}-doped tellurofluorophosphate glasses for lasers and optical amplifiers, J. Phys.: Condens. Matter 17 (2005) 7705–7715.
[36] J. Tauc, R. GrigorovicI, A. Vancu, Optical properties and electronic structure of amorphous germanium, Phys. Stat. Sol. 15 (1966) 627–637.
[37] E.A. Davis, N.F. Mott, Conduction in non-crystalline systems V. Conductivity, optical absorption and photoconductivity in amorphous semiconductors, Philos. Mag.: J. Theor. Exp. Appl. Phys. 22(8) (179) (1970) 903–922.
[38] S.H. Wemple, M. DiDomenico Jr., Behavior of the electronic dielectric constant in covalent and ionic materials, Phys. Rev. B 3 (4) (1971) 1338–1351.
[39] K. Venkata Krishnaiah, G. Venkataiah, J. Marques-Hueso, P. Dharmaiah, C.K. Jayasankar, B.S. Richard, Broadband near-infrared luminescence and visible upconversion of Er3+-doped tungstate-tellurite glasses, Sci. Adv. Mater. 7 (2) (2015) 344–353.
[40] K. Venkata Krishnaiah, J. Marques-Hueso, K. Suresh, G. Venkataiah, B.S. Richards, C.K. Jayasankar, Spectroscopy and near infra-red upconversion of Er^{3+}-doped TZNT glasses, J. Luminescence 169 Part A (2016) 270–276.
[41] K. Venkata Krishnaiah, P. Venkata Lakshmamma, Ch. Basavapoornima, I.R. Martín, K. Soler-Carracedo, M.A. Hernández-Rodríguez, V. Venkatramu, C.K. Jayasankar, Er^{3+} -doped tellurite glasses for enhancing a solar cell photocurrent through photon upconversion upon 1500 nm excitation, Mater. Chem. Phys. 199 (2017) 67–72.
[42] Huiyan Fan, Guonian Wang, Kefeng Li, Hu Lili, Broadband 1.5-μm emission of high erbium-doped Bi_2O_3-B_2O_3-Ga_2O_3 glasses, Solid State Commun. 150 (2010) 1101–1103.
[43] C.C. Santos, I. Guedes, C.-K. Loong, L.A. Boatner, A.L. Moura, M.T. de Araujo, C. Jacinto, M.V.D. Vermelho, Spectroscopic properties of Er^{3+}-doped lead phosphate glasses for photonic Application, J. Phys. D: Appl. Phys. 43 (2010) 025102.